Journal of Ovarian Research

RESEARCH

Open Access

Zishen Yutai pill ameliorates ovarian reserve by mediating PI3K-Akt pathway and apoptosis level in ovary

Jianzhao Chen[1†], Nannan Wang[2†], Zilun Peng[1], Xiufei Pang[2], Na Ning[2], Qingyun Du[1], Qiuping Guo[1*] and Qiuling Huang[2*]

Abstract

Zishen Yutai Pill (ZYP) is a widely used Chinese patent medicine in the clinical treatment of diminished ovarian reserve (DOR) induced infertility in China. However, the pharmacological actions and underlying mechanisms of ZYP in treating DOR remain poorly understood. This study aimed to evaluate the therapeutic effects of ZYP on DOR and elucidate its potential mechanisms. Two models including tripterygium glycosides (TGs)-induced DOR rat model and pZP3-induced DOR mouse model were selected to assess the effectiveness of ZYP in treating DOR. The intervention lasted for 4 weeks in both models. ZYP administration significantly increased the primordial follicles and the serum levels of AMH both in DOR rat and mouse model. Further, ZYP regulated the apoptosis pathway and apoptosis-related molecules including PI3K-Akt signaling pathway, Bcl6 and Abtb2 in ovary of DOR rat. The ovarian apoptosis level was significantly downregulated in a dose-depended manner in ZYP groups. Thus, we demonstrate that ZYP improved the ovarian reserve in DOR models. The mechanisms of ZYP on DOR may be mediated through decreasing the apoptosis level by the regulation of PI3K-Akt signaling pathway and apoptosis molecules (Bcl6, Abtb2) in ovary.

Keywords Zishen Yutai Pill (ZYP), Diminished ovarian reserve (DOR), PI3K/Akt, Apoptosis

Introduction

The ovarian reserve is a key indicator of female fertility, reflecting the quantity and quality of oocytes available for reproduction [1]. Diminished ovarian reserve (DOR) is a disorder of ovarian function characterized by a decrease in the number and/or quality of oocytes [2], which contributes significantly to female infertility. Female ovarian reserve has been reported to decline progressively with advancing age [3], environmental pollution [4], stress [5], and illnesses [6]. In clinical practice, various factors were used in the prediction of ovarian reserve, including age, antral follicle count (AFC), basal sex hormone level, etc. [7] Among them, AFC and anti-Mullerian hormone (AMH) are now widely acknowledged as the most reliable predictors [8].

DOR is responsible for approximately 20% of ovarian-related conditions in women. Within the infertile population, its prevalence is estimated to be around 10%. The incidence of DOR is rising annually, and there is a notable trend of younger patients being affected [9, 10]. Currently, the therapy for DOR in clinical include hormone replacement therapy (HRT), dehydroepiandrosterone (DHEA) supplementation, ovulation induction therapy, assisted reproductive technology (ART), ovum

†Jianzhao Chen and Nannan Wang contributed equally to this work.

*Correspondence:
Qiuping Guo
vipvivenguoguo@126.com
Qiuling Huang
huangqiuling1982@163.com
[1] Center for Drug Non-Clinical Evaluation and Research, Guangzhou General Pharmaceutical Research Institute Company Limited, Guangzhou, Guangdong 510240, People's Republic of China
[2] Guangzhou Baiyunshan Zhongyi Pharmaceutical Company Limited, Guangzhou, Guangdong 510530, People's Republic of China

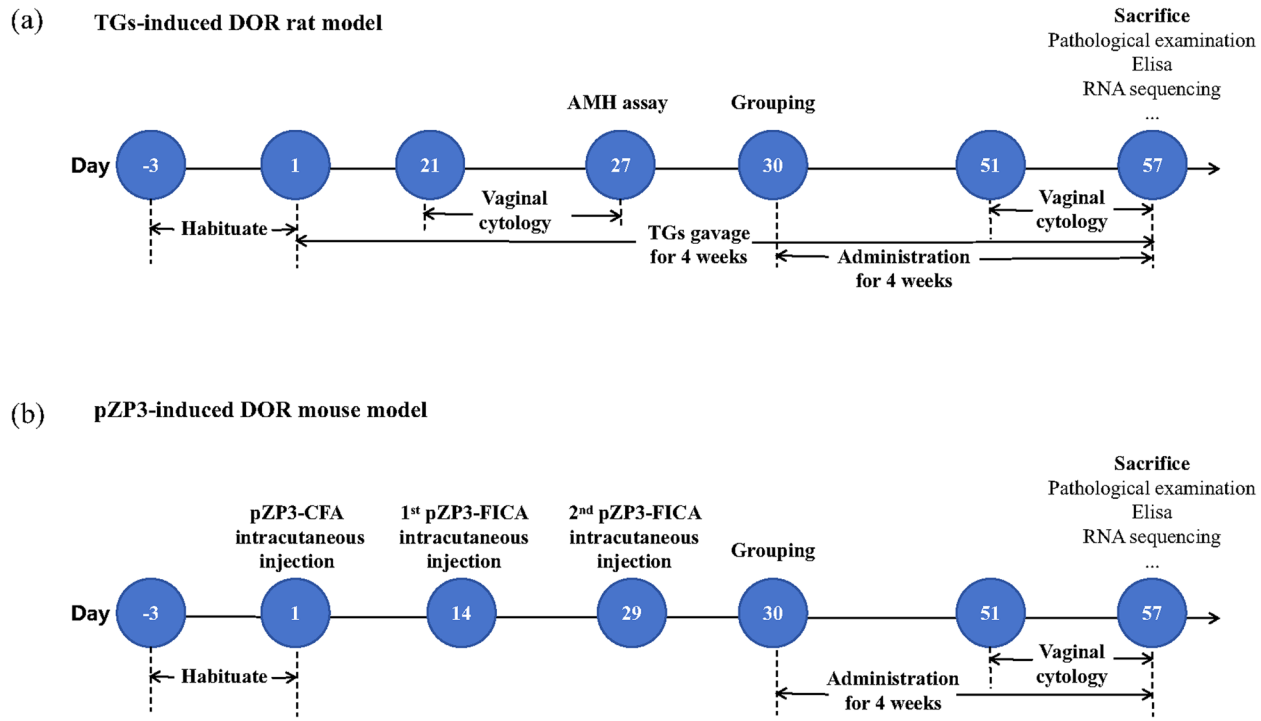

Fig. 1 Timeline of animal experiment procedures. **a** The procedures for modeling, administration, and testing in DOR rat model. **b** The procedures for modeling, administration, and testing in DOR mouse model

donation, and ovarian transplantation [11, 12]. However, the current therapeutic methods are still unsatisfactory. Long-term application of HRT increased the risk of stroke, cardiovascular disease, breast cancer, and venous thromboembolism [13]. The efficacy of DHEA is also a matter of debate [14], despite evidence from animal studies showing its potential to mitigate DOR severity and enhance ovarian reserve function [15]. Furthermore, the safety profile of DHEA supplementation requires further investigation [16]. Ovulation induction therapy is clinically suboptimal for patients with DOR due to poor ovarian response and compromised oocyte quality [17]. Other treatments such as ovum donation and ovarian transplantation are also limited by ethical, moral, and legal concerns [18]. Therefore, developing a medicine treating DOR is considered to be one of the most challenging tasks.

Traditional Chinese Medicine (TCM) has emerged as a potential alternative, demonstrating beneficial effects on ovarian function and infertility management in both clinical and preclinical studies [19, 20]. Zishen Yutai Pill (ZYP) is a well-known mixed herbal medicine composed of fifteen medicine materials, including Rehmanniae Radix Preparata, Ammomi Fructus, Cuscutae Semen, Ginseng Radix, Taxilli Herba, Polygoni multiflori Radix, Artemisiae argyi Folium, Morindae officinalis Radix, Atractylodis macrocephalae Rhizoma, Codonopsis Radix, Lycii Fructus, Dipsaci Radix, Eucom- miae Cortex, Asini Corii Colla, and Cervi Cornu Degelatinatum [21–23]. ZYP is widely applied in reproductive disorders, including infertility, miscarriage, recurrent spontaneous abortion, menstrual disorder, luteal dysfunction, polycystic ovary syndrome etc. [21] Although ZYP are traditionally known to improve ovarian reserve, evidences supporting its efficacy in DOR remains limited.

In this study, we investigated the effects of ZYP administration on ovarian reserve in rats and mice over a 4-week period. Additionally, we explored the underlying mechanisms through which ZYP mitigates ovarian functional decline in these models using transcriptomic analysis.

Results

Effects of ZYP on estrous cycles

The specific time points for modeling, administration and detection of DOR rats are shown in Fig. 1. Vaginal cytology was employed to monitor the changes in the estrus cycles.

After the 28 days administration, metestrus prolonged and diestrus phase decreased in DOR rats (Fig. 2a). ZYP could not reversed this trend. When treated with ZYP, 50% to 80% of rats showed regular estrous cycles

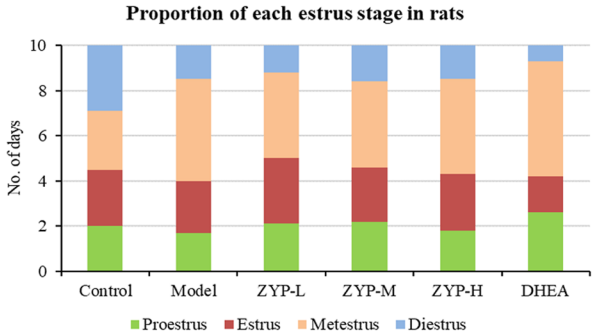

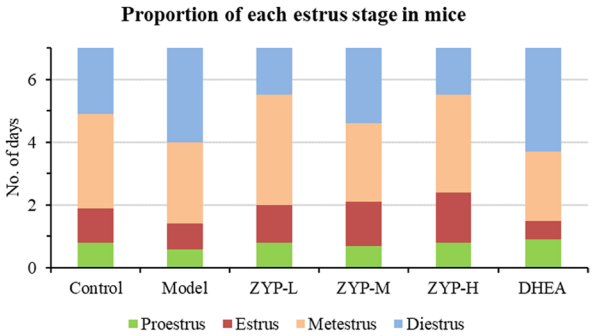

Group	Estrus stage in rats			
	Proestrus	Estrus	Metestrus	Diestrus
Control	2.0±0.8	2.5±0.6	2.6±1.7	3.0±1.9
Model	1.7±1.0	2.3±0.6	4.5±1.3$^{\#\#\#}$	1.6±1.1$^{\#\#}$
ZYP-L	2.1±0.6	2.9±1.3	3.8±1.7$^{\#}$	1.4±1.3$^{\#\#\#}$
ZYP-M	2.2±1.0	2.4±1.2	3.8±1.7$^{\#}$	1.7±1.4$^{\#\#}$
ZYP-H	1.8±1.0	2.5±0.8	4.2±1.5$^{\#\#}$	1.6±1.1$^{\#\#}$
DHEA	2.6±1.8	1.6±1.0$^{\#\#*}$	5.1±1.8$^{\#\#\#}$	0.8±1.0$^{\#\#\#}$

(a)

Group	Estrus stage in mice			
	Proestrus	Estrus	Metestrus	Diestrus
Control	0.8±0.6	1.1±0.7	3.0±1.6	2.2±1.2
Model	0.6±0.5	0.8±1.0	2.6±1.4	3.1±1.9
ZYP-L	0.8±0.7	1.2±0.9	3.5±1.2	1.5±1.3*
ZYP-M	0.7±0.6	1.4±1.4	2.5±1.0	2.4±1.5
ZYP-H	0.8±0.6	1.6±1.1	3.1±1.4	1.6±1.2*
DHEA	0.9±0.9	0.6±0.8	2.2±1.5	3.5±2.1

(b)

Fig. 2 Representative number of days in each estrus stage. **a** The observation of estrus stages in rats began on the 19th day of the experiment and was continually performed once a day for 10 consecutive days and ended on the 28th day. #$P<0.05$, ##$P<0.01$ and ###$P<0.001$, compared with the control group; *$P<0.05$, compared with the model group ($n=20$). **b** The observation of estrus stages in mice began on the 22nd day of the experiment and was continually performed once a day for 10 consecutive days and ended on the 28th day. *$P<0.05$, compared with the model group ($n=20$). Data are presented as mean ± standard deviation of the mean

Table 1 Changes in estrus stages in the rats

Group	N	Normal (N)	Irregular (N)	The rate of regulars (%)
Control	20	20	0	100
Model	20	7	13	35$^{\#\#}$
ZYP-L	20	10	10	50$^{\#\#}$
ZYP-M	20	13	7	65$^{\#\#}$
ZYP-H	20	16	4	80$^{\#**}$
DHEA	20	10	10	50$^{\#\#}$

$^{\#}$ $P<0.05$, ##$P<0.01$, compared with the control group. **$P<0.01$, compared with the model group. Irregular is defined as estrus stages that lasted > 6 days or estrus cycles could not be observed

Table 2 Changes in estrus stages in the mice

Group	N	Normal (N)	Irregular (N)	The rate of regulars (%)
Control	20	18	2	90
Model	20	4	16	20$^{\#\#}$
ZYP-L	20	8	12	40$^{\#\#}$
ZYP-M	20	11	9	55$^{\#*}$
ZYP-H	20	13	7	65**
DHEA	20	9	11	45$^{\#\#}$

$^{\#}$ $P<0.05$, ##$P<0.01$, compared with the control group. **$P<0.05$, **$P<0.01$, compared with the model group. Irregular is defined as estrus stages that lasted > 6 days or estrus cycles could not be observed

(Table 1). The percentage of regular estrus cycles in ZYP-H group was significantly higher than that of the model group ($P<0.01$).

Compared with the control group, the diestrus of DOR mice was prolonged but without significant difference (Fig. 2b). Treatment with ZYP significantly reduced the duration of diestrus compared to the model group in both ZYP-L and ZYP-H groups. Among ZYP-treated mice, 40% to 65% exhibited regular estrous cycles (Table 2). The percentage of regular estrus cycles in ZYP-M group and ZYP-H group was significantly higher than that of the model group ($P<0.05$ or $P<0.01$).

The results indicated that TGs or pZP3 had negative effects on ovarian function, and ZYP effectively mitigates this damage.

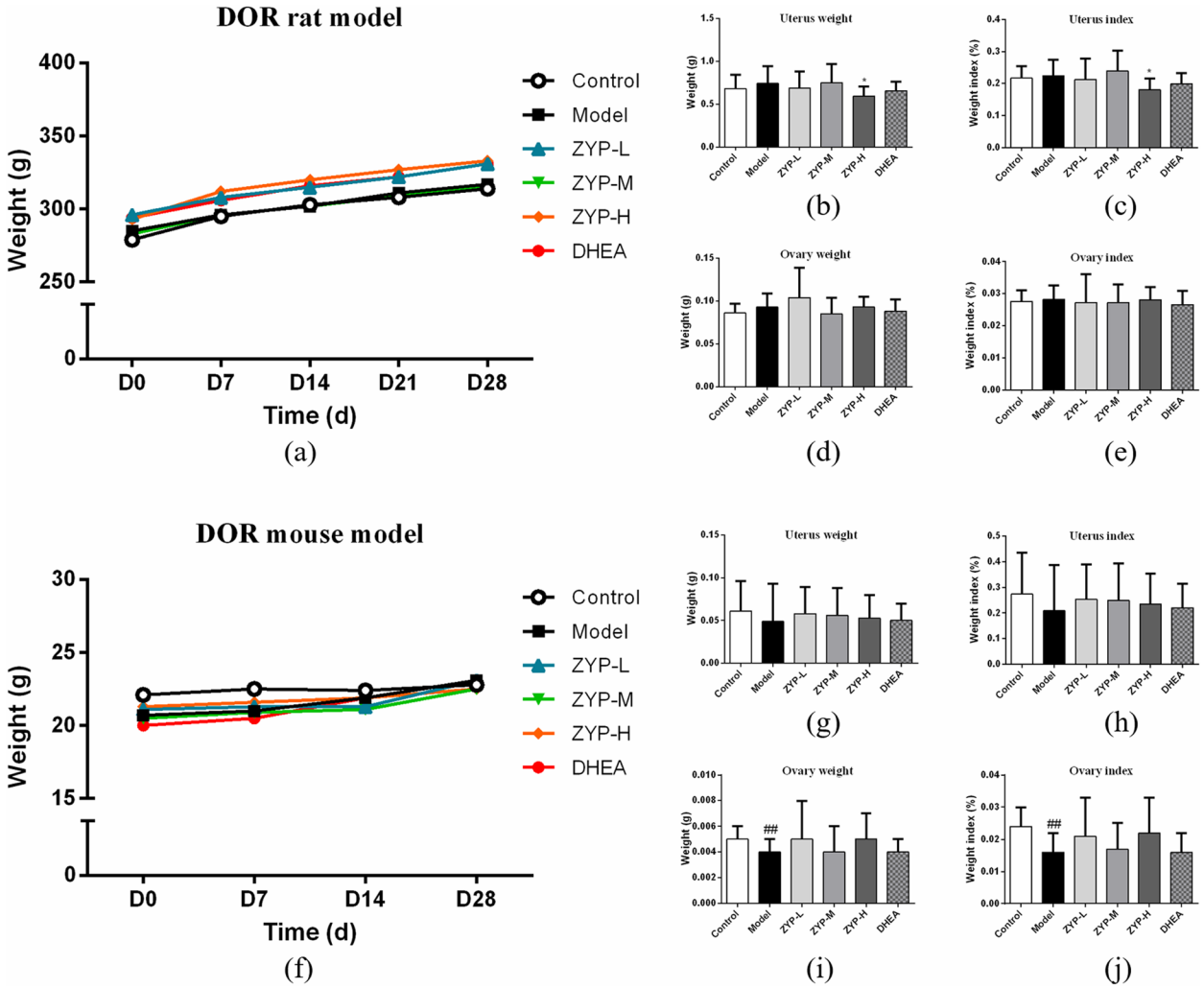

Fig. 3 Body weight and reproductive organs weight changes in rats and mice after ZYP administration ($n = 20$). **a** Body weight changes of rats in each group during experimental manipulation. **b**-**c** Uterus weight and uterus weight index of rats in each group. $^{*}P < 0.05$, compared with the model group. **d**-**e** Ovarian weight and ovarian weight index of rats in each group. **f** Body weight changes of mice in each group during experimental manipulation. **g**-**h** Uterus weight and uterus weight index of mice in each group. **i**-**j** Ovarian weight and ovarian weight index of mice in each group. $^{\#\#}P < 0.01$, compared with the control group. Data are presented as mean ± standard deviation of the mean

General condition and observation of reproductive organs

To adjust the dose of ZYP or DHEA, body weight changes in rats and mice from different groups were monitored every 7 days throughout the 28-day manipulation. As Fig. 3a and b shows, no significant differences were observed between the groups during drug administration. This indicates that ZYP and DHEA do not affect the body weight of rats and mice.

After 28 days of ZYP administration, the uterus weight and index in the ZYP-H group were significantly decreased compared to the model group in DOR rat model (Fig. 3b and c, $P < 0.05$). However, no significant differences were observed among the groups in ovarian weight or ovarian index (Fig. 3d and e).

In DOR mouse model, the ovarian weight and index of in the model group was significantly decreased compared to the control group (Fig. 3i and j), indicating ovarian damage induced by pZP3. After ZYP treatment, the ovarian weight and index exhibited a trend of increase, although this change did not reach statistical significance.

Ovarian reserve changes after ZYP treatment

To investigate the effects of ZYP on different stages of follicles and the corpus luteum, the ovaries of morphological alterations were observed.

Representative microscopic view of ovarian HE staining in DOR rats are shown in Fig. 4a. Compared with the control group, the model group exhibited a significant

decrease in the numbers of primordial and secondary follicles ($P<0.05$) but a significant increase in the number of antral follicles ($P<0.05$). While the trend in the ZYP-M and ZYP-H groups was reversed in a dose-dependent manner compared to the model group (Fig. 4b). In addition, the number of corpora lutea was significantly increased in ZYP-M and ZYP-H groups in a dose-dependent manner compared to the model group ($P<0.05$). These results suggest that ZYP administration effectively prevents the depletion of the primordial follicle pool in the DOR rat model.

The number of ovarian follicles at different stages and the number of corpora lutea in mice were shown in Fig. 4c. Compared with the control group, the model group exhibited a significant decrease in the numbers of primordial follicles and corpora lutea ($P<0.05$) but a significant increase in the number of secondary follicles ($P<0.05$). Compared with the model group, the numbers of primordial follicles and corpora lutea in ZYP-M and ZYP-H groups were significantly increased ($P<0.05$). These results suggest that ZYP administration effectively prevents the depletion of the primordial follicle pool in DOR mouse model.

Effects of ZYP on serum hormones

As shown in Fig. 5, the levels of AMH and E2 in DOR rats were significantly decreased compared to the control group after model establishment. After 28 days of treatment, the model group exhibited a significant reduction in AMH levels compared to the control group ($P<0.01$). In contrast, AMH levels were significantly elevated in the ZYP-H and DHEA groups compared to the model group ($P<0.01$). Compared with the control group, rats in the model group showed markedly lower serum levels of E2 and considerably higher serum levels of FSH and LH ($P<0.05$, $P<0.01$ or $P<0.01$). The serum level of E2 was decreased significantly in the ZYP-H compared to the model group ($P<0.05$). The serum FSH and LH levels were significantly suppressed in the ZYP-L, ZYP-M, ZYP-H and DHEA groups compared to the model group ($P<0.05$, $P<0.01$ or $P<0.01$).

As shown in Fig. 6, AMH levels of DOR mice were significantly decreased compared to the control group after model establishment. After 28 days of treatment, the model group exhibited a significant reduction in AMH levels compared to the control group ($P<0.05$). In contrast, AMH levels were significantly elevated in the ZYP-H and DHEA groups compared to the model group ($P<0.05$). Compared to the control group, mice in the model group showed markedly lower serum levels of E2 and LH and considerably higher serum levels of FSH/LH ($P<0.05$). The serum E2 and LH levels were elevated significantly in the ZYP-H and DHEA groups compared to the model group ($P<0.05$). The serum FSH/LH levels were significantly suppressed in the ZYP-M, ZYP-H and DHEA groups compared to the model group ($P<0.05$).

ZYP reversed TGs-induced changes in mRNA expression in rat ovaries

Messenger RNA (mRNA) sequencing was performed to compare the mRNA expression patterns in ovulated ovaries obtained from control, model, and ZYP-H groups rats. Hierarchical clustering analysis revealed 703 differentially expressed genes (DEGs) in the three groups, with fold changes ≥ 1.5 or $\leq 2/3$ ($P<0.05$, Fig. 7a).

Comparison of the model and control rats data revealed 255 differentially upregulated genes and 285 downregulated genes. Comparison of the ZYP-H and model rats data revealed 95 differentially upregulated genes and 68 downregulated genes (Fig.7b). ZYP administration induces different changes in mRNA expression in the ovary.

Bioinformatic analysis was performed for all the DEGs. Kyoto Encyclopedia of Genes and Genomes pathway analysis of DOR rats datasets revealed that the DEGs were involved in the PI3K-Akt signaling pathway (Table 3). Expression of five genes associated with the PI3K-Akt signaling pathway including phosphoinositide-3-kinase regulatory subunit 5 (Pik3r5), retinoid X receptor alpha (Rxra), nuclear receptor subfamily 4 group A member 1 (Nr4a1), G protein subunit beta 3 (Gnb3), T-cell leukemia/lymphoma 1A (Tcl1a), heat shock protein 90 alpha family class A member 1 (Hsp90aa1) and two apoptosis molecules genes including B-cell CLL/lymphoma 6B (Bcl6) and ankyrin repeat and BTB domain containing 2 (Abtb2) was analyzed. In the model group, the genes include Pik3r5, Gnb3, Tcl1a, Bcl6, Abtb2 were upregulated and Rxra was downregulated (Figs. 8 and 9). Compared with the model group, Nr4a1 was upregulated, and Hsp90aa1, Bcl6, Abtb2 were downregulated.

(See figure on next page.)

Fig. 4 ZYP improved ovarian reserve in DOR. **a** H&E staining of ovarian tissues in the indicated groups (×20, ×100, ×200 magnification). **b** Number of ovarian follicles in different stages and the number of corpora lutea in rats. #$P<0.05$, compared with the control group; *$P<0.05$, **$P<0.01$ and ***$P<0.001$, compared with the model group ($n=12$). **c** Number of ovarian follicles in different stages and the number of corpora lutea in mice. #$P<0.05$, compared with the control group; *$P<0.05$, compared with the model group ($n=12$). Data are presented as mean ± standard deviation of the mean

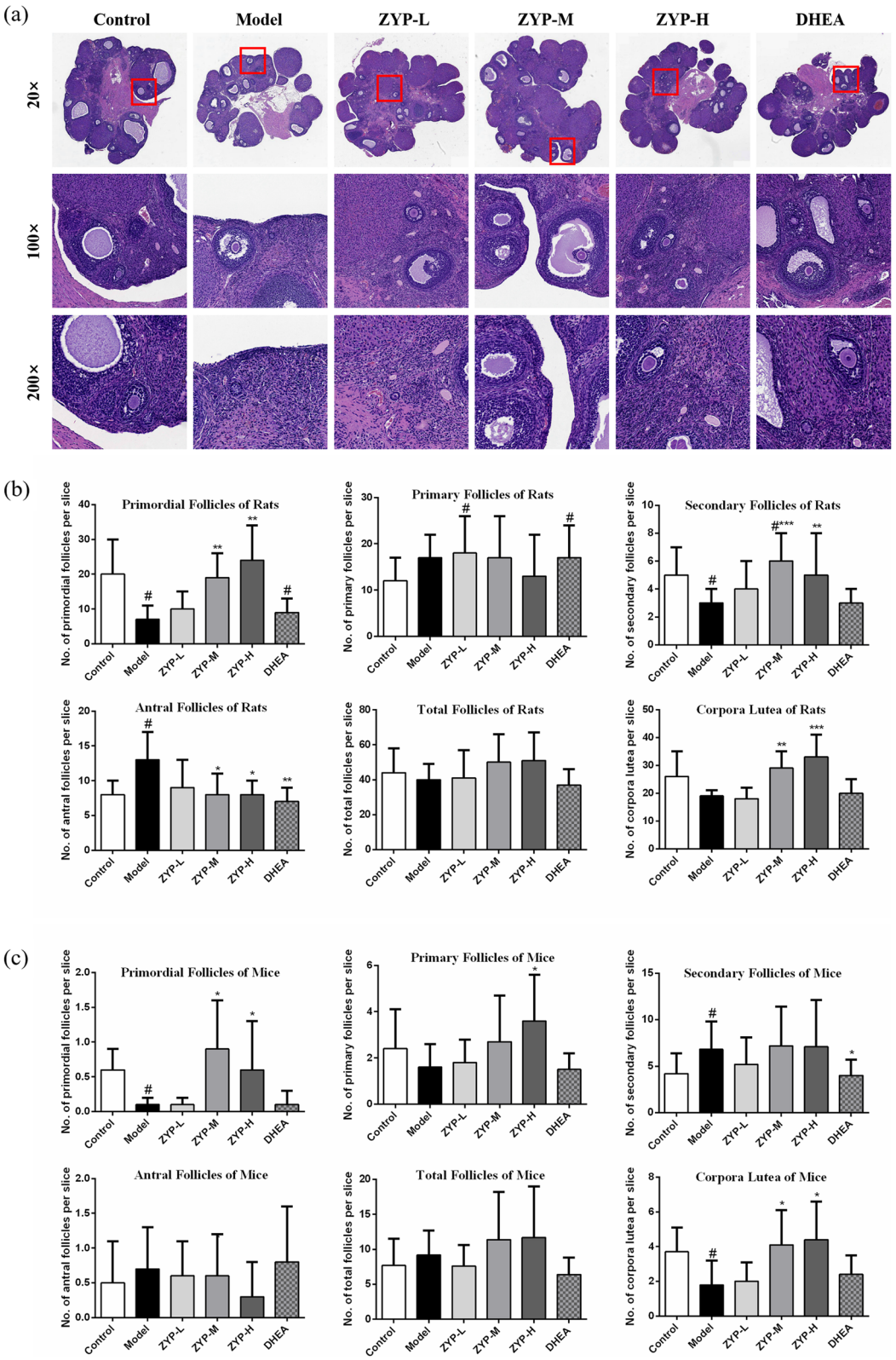

Fig. 4 (See legend on previous page.)

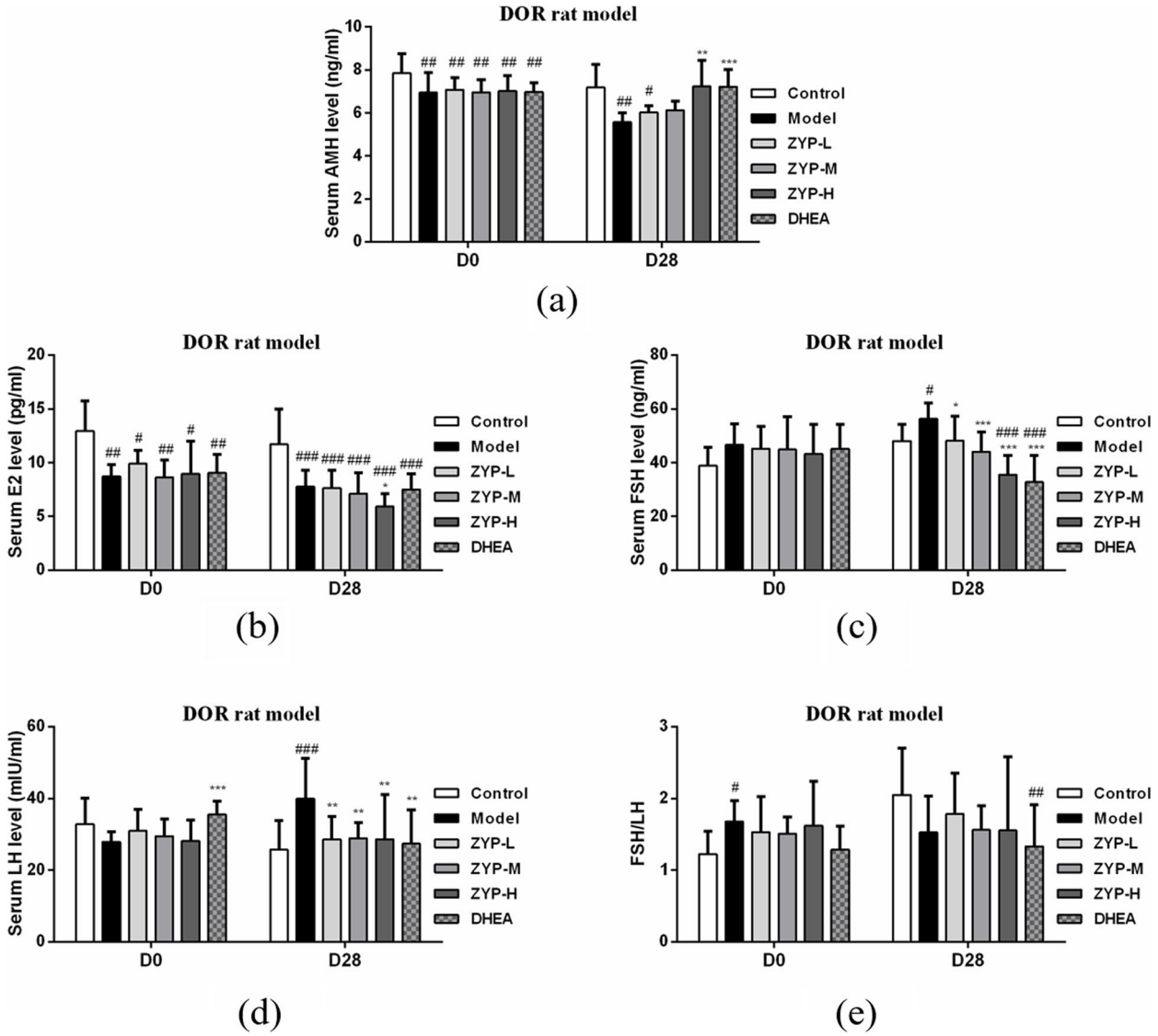

Fig. 5 Serum hormone levels in DOR rat model. **a** AMH, **b** E2, **c** FSH, **d** LH, **e** FSH/LH. #$P < 0.05$, ##$P < 0.01$ and ###$P < 0.001$, compared with the control group; *$P < 0.05$, **$P < 0.01$ and ***$P < 0.001$, compared with the model group ($n = 12$). Data are presented as mean ± standard deviation of the mean

The mRNA expression trends of PI3K-Akt signaling pathway and two apoptosis molecules genes were consistent with their qRT-PCR results. These observations indicated that ZYP could regulate the PI3K-Akt signaling pathway and apoptosis molecules genes including Bcl6 and Abtb2 in the ovarian tissue of DOR rats.

ZYP reduces ovary cell apoptosis in DOR rats

To further confirm whether ZYP affects the apoptotic level of the ovary, we conducted an additional test using a Cell Death Detection ELISA (Roche, cat# 11,544,675,001), which determines histone-associated DNA fragments generated by apoptotic cell death. Ovarian tissue lysates were collected from rats and processed separately for analysis. The data shows that TGs significantly increased the level of apoptotic cell death in DOR rat ovaries. However, ZYP administration effectively restored the apoptotic level in a dose-dependent manner (Fig. 10). This finding suggests that ZYP can mitigate the apoptotic effects induced by TGs in the ovarian tissue of DOR rats.

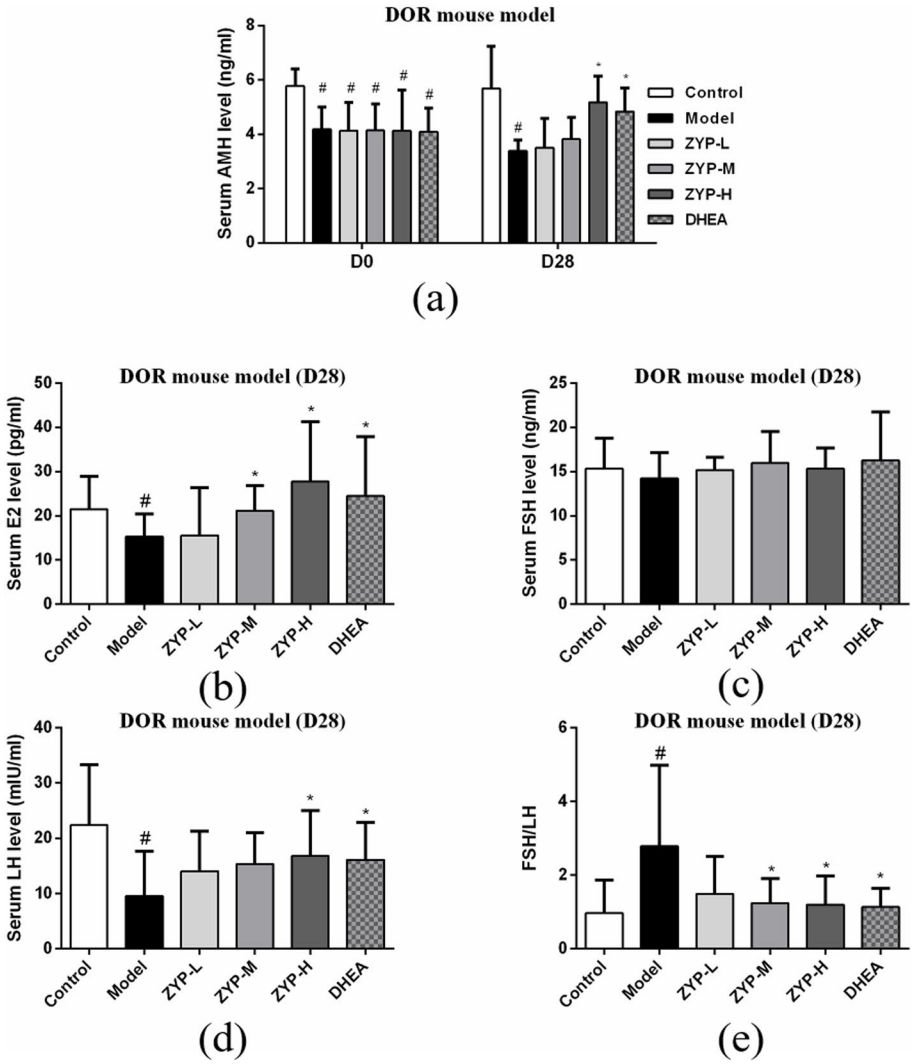

Fig. 6 Serum hormone levels in DOR mouse model. **a** AMH, **b** E2, **c** FSH, **d** LH, **e** FSH/LH. #$P < 0.05$, compared with the control group; *$P < 0.05$, compared with the model group ($n = 12$). Data are presented as mean ± standard deviation of the mean

Discussion

DOR is a complex gynecological endocrine disease that increases the incidence of the poor ovarian response, decreases the embryo implantation rates, and diminishes the success rates of assisted reproductive techniques [24]. Thus, improving ovarian reserve is crucial for patients seeking pregnancy. TCM provides an alternative strategy in the treatment of DOR.

In clinical practice, ZYP exhibited promising efficacy and safety in the management of infertility [25]. The present study investigated the protective effect of early intervention with ZYP on DOR induced by TGs in rats and pZP3 mixture in mice, aiming to elucidate its potential benefits in clinical DOR treatment.

Previous studies have demonstrated that TGs causes premature ovarian insufficiency by inducing death and/or by accelerating activation of primordial follicles and increasing atresia of growing follicles [26, 27]. It also changes the apoptotic in granulosa cells and leads to follicle loss [28]. Data showed the pZP3 mixture causes premature ovarian failure by stimulating the immune system to secrete anti-pzp3 antibody, resulting in accelerated destruction and depletion of oocytes [29]. Therefore, the toxic effects of TGs or pZP3 mixture on the female reproductive system can be utilized to induce animal models of DOR. These two models have been used in previous studies. In this study, a 90 mg/kg dose of TGs was used to establish a DOR rat model, and a 200 μl dose of pZP3

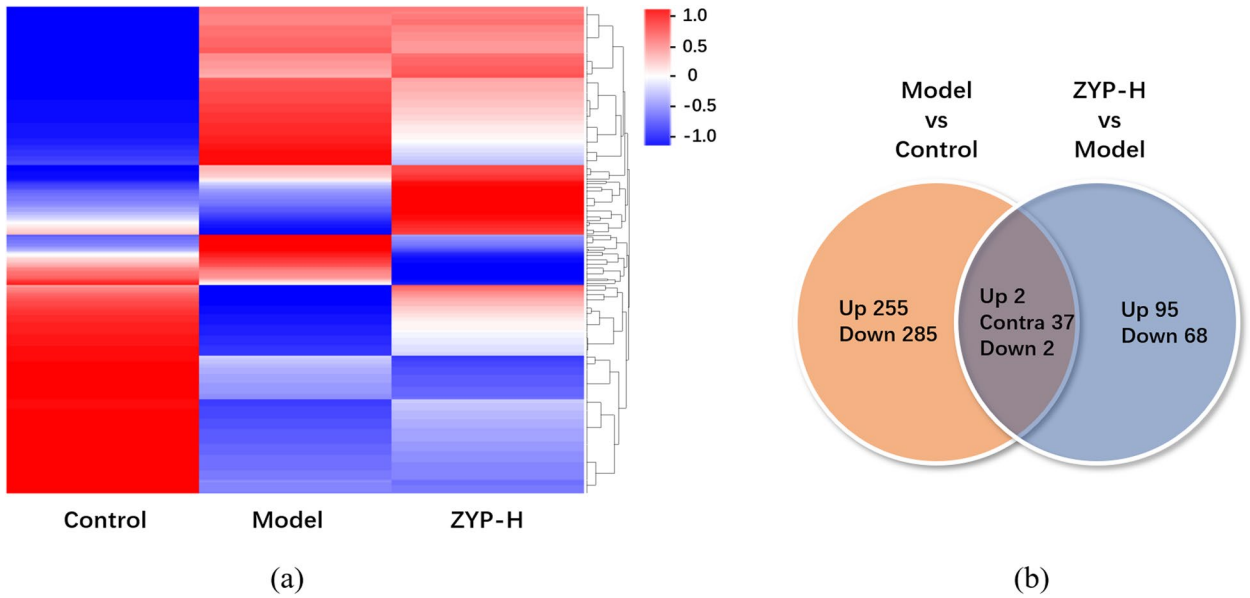

Fig. 7 Hierarchical clustering and analysis of differentially expressed mRNAs. Messenger RNA analysis was performed to compare the gene expression in ovulated ovaries of control ($n=5$), model ($n=5$), and ZYP-H ($n=5$) rats. **a** Hierarchical clustering among the mRNA expression profiles showing 703 differentially expressed mRNAs in the three groups, with fold changes ≥ 1.5 or ≤ 2/3 and $P<0.05$. Red denotes upregulation of gene expression and blue denotes downregulation of gene expression. **b** Venn diagram presenting the numbers of differentially expressed mRNAs between model vs. control and ZYP-H vs. model pairs. Up, upregulated genes between compared sets; Contra, contra regulated genes between compared sets; Down, downregulated genes between compared sets

Table 3 Functional annotation of differentially expressed genes

Term	*P*-value	Genes
rno04060:Cytokine-cytokine receptor interaction	8.31E-05	Pf4, Il23a, Il23r, Ccl3, Ccr7, Gdf15, Ccl7, Lifr, Tnfrsf9, Inhba, Bmpr1b, Ebi3, Tnfrsf25, Il2ra, Ccl21, Cxcl13, Tnfrsf4, Il15raLif, Tnfrsf18
rno04151:PI3K-Akt signaling pathway	0.0198	Ereg, Comp, LOC103692716, Pik3r3, **Hsp90aa1**, Angpt1, Pck1, Areg, Tgfa, **Nr4a1**, Tnc, Gm45713, **Gnb3**, Col4a3, Il2ra, **Pik3r5**, Itgb3, **Rxra, Tcl1a**
rno04012:ErbB signaling pathway	0.0351	Ereg, Pak3, Pik3r3, Gab1, Areg, Tgfa

Kyoto Encyclopedia of Genes and Genomes analysis was performed to identify the potential signaling pathway of the differentially expressed genes

mixture was used to establish a DOR mouse model. Our results also demonstrated that the administration of TGs or pZP3 mixture provoked ovarian damage, as evidenced by reduced follicular counts, and impairment of hormonal regulation. These results are in consistent with previous studies demonstrating follicular damage from TGs or pZP3 mixture. Subsequently, the effects of different doses of ZYP on these models were examined.

AFC and AMH are well-established predictors of ovarian function [8]. In this study, ZYP administration significantly increased the numbers of primordial follicles, secondary follicles and corpora lutea, whereas that of atretic follicles was reduced, compared with DOR rats. Similar therapeutic effects were also observed in DOR mice. This evidence demonstrated that ZYP significantly improved folliculogenesis and ovulation in DOR models. AMH is secreted by granulosa cells of growing follicles [30]. It is strongly correlated with AFC and represents a reliable biomedical marker of ovarian reserve [31]. Previous reports have reported that TGs or pZP3 mixture decreased the serum AMH levels [32, 33]. In our research, high-dose ZYP treatment significantly reversed this effect, suggesting that ZYP protects ovarian granulosa cells and preserves ovarian reserve function. Taken together, these results indicated that ZYP significantly ameliorated ovarian damage caused by TGs or pZP3 mixture, particularly at high doses.

TGs-induced high levels of FSH and LH in rats led to rapid depletion of the primordial follicle pool and caused DOR [34]. This phenomenon was not observed in the DOR mouse model, as pZP3 mixture-induced damage was primarily through immunoreaction [35]. In this study, after ZYP treatment, FSH and LH levels decreased in DOR rats, suggesting that ZYP's therapeutic effects

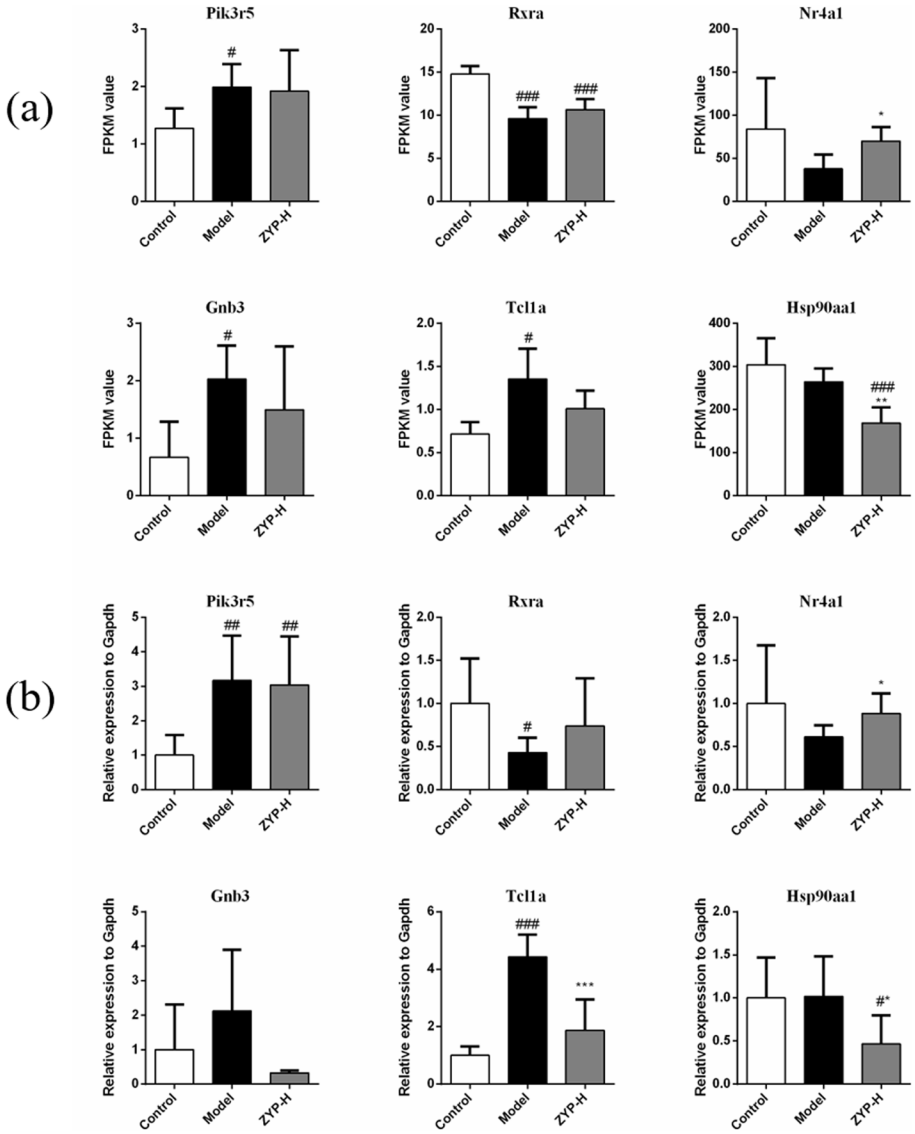

Fig. 8 Differentially expressed mRNAs involved in PI3K-Akt signaling pathway. **a** mRNA sequencing data ($n=5$) and (**b**) validation by qRT-PCR ($n=6$). #$P<0.05$, ##$P<0.01$ and ###$P<0.001$, compared with the control group; *$P<0.05$, **$P<0.01$ and ***$P<0.001$, compared with the model group. Data are presented as mean ± standard deviation of the mean

may involve regulation of gonadal hormones, thereby improving ovarian reserve function.

Messenger RNA sequencing and qRT-PCR results showed that the DEGs were involved in the PI3K-Akt signaling pathway. The PI3K-Akt signaling pathway could regulate the process of cell metabolism, proliferation, differentiation and survival. It is abnormally expressed in tumors, autoimmune diseases, fibroproliferative diseases and other pathema [36]. Intact PI3K Akt signaling pathway exists in both oocytes and granulosa cells. They jointly regulate the initiation and survival of follicles [37]. PI3K-Akt signaling pathway is also involved in oocyte growth and granulosa cell proliferation and apoptosis [38]. Previous studies have demonstrated that TGs activates the PI3K-Akt pathway, leading to excessive primordial follicle activation and apoptosis [34]. In addition, metabonomics study in IVF-ET patients demonstrated possible effects of ZYP on PI3K-Akt pathway [39]. Our results showed that the expression pattern is significantly changed in the ZYP treatment group, suggesting that ZYP could prevent TGs-induced overactivation of the primordial follicle pool and inhibit cell apoptosis via a PI3K/AKT-dependent mechanism.

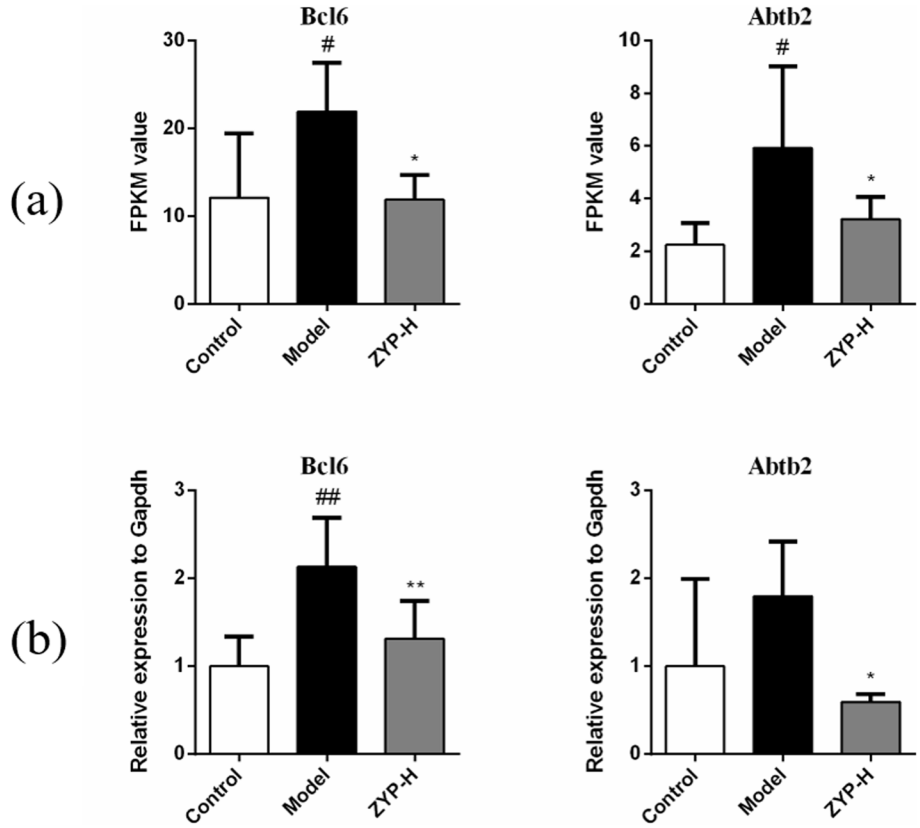

Fig. 9 Differentially expressed mRNAs involved in apoptosis molecules Bcl6 and Abtb2. **a** Messenger RNA sequencing data ($n=5$) and (**b**) validation by qRT-PCR ($n=6$). #$P<0.05$ and ##$P<0.01$, compared with the control group; *$P<0.05$ and **$P<0.01$, compared with the model group. Data are presented as mean ± standard deviation of the mean

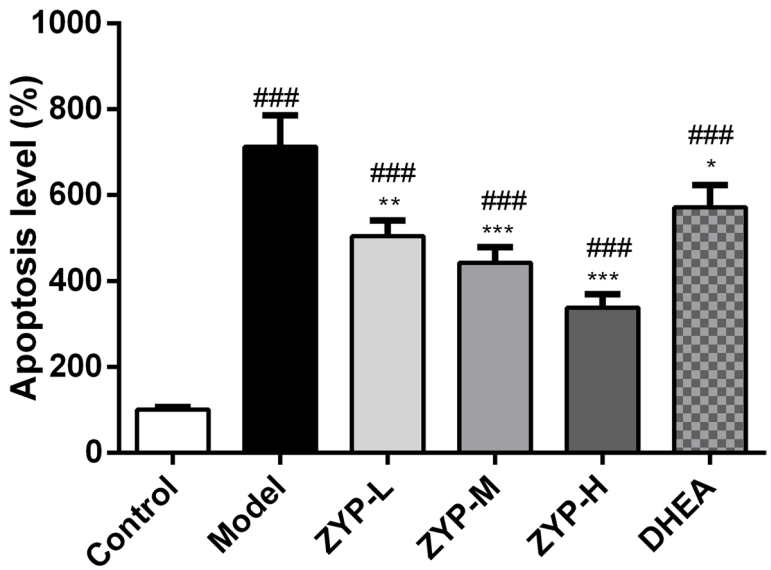

Fig. 10 Effects of ZYP on TGs-induced apoptosis of ovary cell analyzed by a Cell Death Detection ELISA Kit after 28 days treatment. ##$P<0.01$, compared with the control group; *$P<0.05$ and **$P<0.01$, compared with the model group ($n=6$). Data are presented as mean ± standard deviation of the mean

Besides, we found that ZYP could regulate the expression of apoptosis-related genes Bcl6 and Abtb2. Previous studies have demonstrated that overexpression of Bcl-6 induces apoptosis of CV-1 cells and Hela cells. This process is accompanied by downregulation of anti-apoptotic genes Bcl2 and Bcl-xl and upregulation of pro-apoptotic gene Bax [40]. The protein encoded by the ABTB2 gene is ankyrin repeat and BTB/POZ domain-containing protein [41], which participates in the function of regulating cell growth and the degradation of defective proteins, thereby affecting apoptosis [42, 43]. Our data showed that the expression of Bcl6 and Abtb2 were significantly upregulated in the TGs-treated group, but ZYP administration reversed this trend, indicating that ZYP may be a promising protective candidate against TGs-induced apoptosis in the ovarian follicles. Cell Death Detection ELISA confirmed the inhibitory effect of ZYP on apoptosis.

In short, ZYP downregulated the expression of Bcl6 and Abtb2 through PI3K-Akt pathway in ovary, thereby enhancing ovarian reserve. This study provided sound evidences for the treatment of DOR using ZYP. However, several limitations of the study should be acknowledged. The pharmacological mechanisms underlying the efficacy of ZYP are likely to be multifaceted. A network pharmacological study suggested that the mechanism of ZYP in the treatment of DOR may be associated with PI3K/AKT, p53, endocrine resistance and other signaling pathways [44]. ZYP also exhibited amelioration effects of oocyte quality by elevating BMP15 and GDF9 expressions in the follicle fluids [45]. Other mechanisms relating to DOR, for example, cellular senescent and oocyte development, remain to be verified. Moreover, TCM clinical application is fundamentally based on syndrome differentiation and individualized treatment. For instance, ZYP is commonly prescribed for patients presenting with spleen and kidney deficiency (pishenliangxu in Chinese). Although the DOR model induced by triptolide aligns with the TCM syndrome of kidney deficiency, the DOR model employed in this study still cannot fully explain the role of ZYP in clinical practice [46]. However, a large number of research evidences have verified the role of ZYP in the clinical treatment of DOR [47, 48].

Future research should focus on elucidating the comprehensive pharmacological mechanisms of ZYP in DOR, incorporating larger-scale clinical trials and more diverse patient populations to better understand its clinical applicability and therapeutic benefits.

Materials and methods

Chemicals and reagents

Zishen Yutai Pill (ZYP) was obtained from Guangzhou Baiyunshan Zhongyi Pharmaceutical Company Limited (Guangzhou, China). DHEA was obtained from Shanghai Macklin Biochemical Co., Ltd (Shanghai, China). Complete Freund's adjuvant (CFA) was obtained from Sigma (USA). Zona pellucida protein 3 peptides (pZP3) was obtained from ChinaPeptides (Suzhou, China). Tripterygium glycosides (TGs) tablet was obtained from Yuanda Pharmaceutical Huangshi Feiyun Pharmaceutical Co., Ltd (Huangshi, China).

ELISA kits for sexual hormone (AMH, FSH, LH, E2) were obtained from Elabscience (Wuhan, China). Cell death detection ELISA kit was obtained from Roche (Germany).

Trizol reagent was obtained from Ambion (USA). RNA extraction kit was obtained from Tianmo (Beijing, China). SureSelect strand-specific RNA component kit and high sensitivity DNA kit were obtained from Agilent (USA). Qubit dsDNA HS assay kit was obtained from Thermo Fisher (USA). Primers of GAPDH, Hsp90aa1, Pik3r5, Nr4a1, Rxra, Gnb3, Tcl1a, Bcl6, Abtb2 were obtained from Dingguo (Guangzhou, China). Fluorescent quantitative detection kit was obtained from Talent (Beijing, China).

Animals

All animal welfare and experimental procedures were in strict accordance to the Guide for the Care and Use of Laboratory Animals (ethical code number: IA-PD2019006-01, IA-PD2019006-02). SPF grade female Sprague-Daweley (SD) rats (aged 11 weeks, weighing 230–270 g) and BALB/c mice (aged 7 weeks, weighing 18–24 g) were provided by Hunan SJA Animal Company. Animals were housed in SPF animal room of Guangzhou General Pharmaceutical Research Institute Company (GPRI) Center for Drug Non-Clinical Evaluation and Research. The housing environment was maintained at 20–26 ℃, humidity 40–70%. Rats and mice were kept in a 12 h light/12 h dark cycle. Animals were given free access to food and water. At the end of study, all animals were euthanized.

Establishment of the DOR rat model

The DOR model was established by gavage of Tripterygium Glycosides (90 mg/kg) once daily for 4 weeks. Blood samples were collected by tail vein puncture. AMH was measured by ELISA in DOR rats to confirm the successful establishment of the DOR rat model. In the control group, the expression of AMH was higher than that of the DOR rats.

The model rats were randomly divided into 5 groups by the expression of AMH as followed: model group, ZYP-L group (0.68 g/kg/day), ZYP-M group (1.35 g/kg/day), ZYP-H group (2.70 g/kg/day) and DHEA group (0.02 g/kg/day). Control group and model group received 0.5% CMC-Na solution (vehicle of ZYP and DHEA). In the

treatment period, four hour after intragastric administration of TGs, each group had a treatment with vehicle, ZYP, or DHEA.

Four weeks after treatment, rats were anesthetized with 20% urethane (7.5 mL/kg), which was subcutaneously injected. Animals were sacrificed by rapid loss of blood under anesthesia. The blood sample from the abdominal aorta and ovary tissue of each rat were collected for further analysis. The detailed procedures for modeling, administration, and testing in DOR rat model are shown in Fig. 1a.

Establishment of the DOR mouse model

The modified pZP3-induced DOR mice model was established according to the literature [49]. Each mouse was injected intradermally with 200 µl pZP3-CFA (1:1) mixture at back. After 2 weeks, the same volume of pZP3 emulsified in Freund's Incomplete Adjuvant (FICA) (1:1) was injected intradermally. Two weeks following the treatment of pZP3 with FICA, each mouse received another injection with pZP3-FICA (1:1) mixture at back, and blood samples were collected by tail vein puncture. AMH was measured by ELISA in DOR mice to confirm the successful establishment of the DOR mice model. In the control group, the expression of AMH was higher than that of the DOR mice.

The model mice were randomly divided into 5 groups by the expression of AMH as followed: model group, ZYP-L group (0.98 g/kg/day), ZYP-M group (1.95 g/kg/day), ZYP-H group (3.9 g/kg/day) and DHEA group (0.02 g/kg/day). Control group and model group received 0.5% CMC-Na solution (vehicle of ZYP and DHEA). Four weeks after treatment, mice were anesthetized with 20% urethane (7.5 mL/kg), which was subcutaneously injected. Animals were sacrificed by rapid loss of blood under anesthesia. The blood sample from the abdominal aorta and ovary tissue of each mouse were collected for further analysis. The detailed procedures for modeling, administration, and testing in DOR mouse model are shown in Fig. 1b.

Vaginal cytology

Vaginal smears were taken at 8:30 am daily. Cast-off cells were collected to estimate the estrus cycles of mice and rats. The average normal estrus cycle in a rat or mice is 4–5 days, which can be generally divided into four stages: proestrus, estrus, metestrus, and diestrus. Different cell types appear and recede in each stage. Proestrus is characterized by a large number of nucleated epithelial cells and few leukocytes. Estrus presents a large amount of cornified and irregular shaped epithelial cells without nucleus. Metestrus is characterized by a combination of nucleated epithelial cells, anucleated keratinized epithelial cells, and leukocytes. Diestrus is characterized by a large number of leukocytes and a low number of cornified epithelial cells [50].

Weight of body, uterus and ovary

All the rats and mice were weighed before dosing. After administration, the body weight of each animal was recorded weekly throughout the experiment. After 28 days of treatment, the uteruses and ovaries were removed and weighed, and the uterine or ovarian index was calculated as follows: uterine or ovarian index = uterine or ovarian wet weight (g)/body weight (g) × 100%. The uteruses and ovaries were fixed in 4% paraformaldehyde (PFA) for histopathology examination, while the 8 of rat ovaries were snap-frozen in liquid nitrogen and stored at −80℃ until analysis of mRNA expression and apoptosis detection.

Histological observation of morphology, and follicle classification

The uterine and ovarian tissues of rats and mice were fixed in 4% PFA for 24 h at room temperature, followed by standard tissue processing and embedding. Paraffin-embedded tissue was sliced into 4-µm-thick sections and dried overnight at 37 ℃. The sections were then deparaffinized in xylene twice for 10 min each and rehydrated using a graded ethanol series. The sections were then stained with H&E, dehydrated, cleared, and mounted for observation. Digital images of stained sections were captured using a light microscope (DP73, OLYMPUS, Japan) and a digital slice scanning system (PRECICE 600, UNIC TECHNOLOGIES, China).

To assess the whole ovary and classify the follicles, the number of follicles at four stages (primordial, primary, secondary, and antral ovarian follicles), as well as the number of corpora lutea, were counted. Follicles were counted as primordial follicles when the oocyte was surrounded by a single layer of flattened follicular cells. The primary follicle was defined when it presented an enlarged oocyte surrounded by a single layer of cuboidal granulosa cells, and the secondary follicle was considered when it showed an oocyte surrounded by multiple layers of cubic granulosa cells. Antral follicles were defined by the presence of several layers of granulosa cells, an oocyte with a clear nucleus, an antrum, and a theca layer. After ovulation, the granulosa cells of the follicle remnant undergo hypertrophy and hyperplasia, resulting in a mature corpus luteum [19].

Serum hormone detection by ELISA

Rat and mouse blood samples were obtained from the tail vein or abdominal aorta, clotted at room temperature for 2 h, and then centrifuged at 1000 g for 20 min

to collect the serum. Then, AMH, E2, FSH, and LH concentrations were measured using the specific ELISA kits according to the manufacturer's protocols. In brief, 100 μL of each serum or standard was added to each well of a coated 96-well plate and incubated for 90 min at 37 ℃. Then the supernatant was discarded and Biotinylated Antibody was then added immediately and incubated for 60 min at 37 ℃. After the reaction was finished, the wells were washed with buffer for three times, followed by the addition of HRP-conjugate Reagent into each well. After 30 min of incubation at 37 ∘C, the wells were aspirated and washed for five times, and incubated with the substrate solution for 15 min at 37 ∘C. Finally, the stop buffer was added, and concentration was determined by the absorbance of the solution at 450 nm.

Messenger RNA sequencing

Total mRNA was isolated from the ovaries of control group, model group and ZYP-H group using QuickRNA MicroPrep Kits (ZYMO research, California, USA). After concentration and purity testing, total mRNA in each sample was reverse transcribed by oligo T primers to synthesize the first strand of cDNA. Subsequently, the double stranded cDNAs were produced by the reaction of RNase H enzyme, DNA polymerase and T4 ligase. The double-stranded cDNAs were then fragmented by Tn5 enzyme and both ends were subjected to addition of sequencing adapters. The P5 and P7 primers were bound to sequencing adapters at both ends and enriched polymerase chain reaction (PCR) amplifications were subsequently performed. The complete library was sequenced with Illumina NovaSeq 6000.

After filtration of all the reads using FASTQ [51], the clean data were aligned to the *Rattus norvegicus* genome to obtain gene expression data in the form of read counts. The data were normalized by converting the read counts to fragments per kilobase of exon model per million mapped fragments (FPKM) values. The differentially expressed genes (DEGs) were screened out among three groups using the following criteria: |log2 fold change| ≥ 1.5 and the adjusted $P < 0.05$ by comparing the FPKM values. Kyoto Encyclopedia of Genes and Genomes (KEGG) analysis were performed to identify the potential functions and associated pathways of DEGs with corrected P values < 0.05.

Real-time polymerase chain reaction

Total RNA was extracted from rat ovaries using TRIzol reagent (Ambion, USA). The cDNAs were generated using PrimeScript™ RT reagent Kit with gDNA Eraser (Takara Bio, Beijing, China) according to the manufacturers' instructions. Quantitative real-time PCR was performed using real-time fluorescence quantitative PCR Systems (DA7600, DaAn Gene, China). Each sample was analyzed for 3 times. The primer sequences for target genes are listed in Table 4. The parameters for qRT-PCR were set as follows: initial denaturation for 3 min at 95 °C followed by 40 cycles of 5 s each at 95 °C, 15 s at 60 °C. The relative gene expression was calculated using the $2^{-\Delta\Delta CT}$ method. Ratios of gene expression were displayed as fold-change relative to the control group after normalizing to the allogeneic glyceraldehyde-3-phosphate dehydrogenase (GAPDH) housekeeping gene.

Table 4 Primer sequences for real-time reverse transcription-polymerase chain reaction

Gene		Primer sequence (5′–3′)	Length (bp)
Pik3r5	Forward	CTCATGCATCTGCCTCCTGAAGT	52
	Reverse	ATTCTGCCTTGAGGGACTGCT	
Rxra	Forward	AACCCCCTCTAGGCCTCAAT	118
	Reverse	TAGTGTTTGCCTGAGGAGCG	
Nr4a1	Forward	GCGAAAGTTGGGGTAGTGTG	126
	Reverse	CTTGGATACAGGGCATCTCCG	
Gnb3	Forward	ATGTGAGGGAAGGGACCTGT	158
	Reverse	GTAGGCTGTCAGTTCCTGGTC	
Tcl1a	Forward	TTGGTTGGCCCTTCCACTCT	111
	Reverse	CTGAGAAGATCAGAGGTGCAGAC	
Hsp90aa1	Forward	ATGATGACGAGCAGTACGCC	79
	Reverse	CCCATTGGTTCACCTGTGTCT	
Bcl6	Forward	TATGGAGCCTGCGAACCTTG	163
	Reverse	GTGCATGTAGAGTGGCGAGT	
Abtb2	Forward	TAGGCCTTCTGGGGTAGGCT	149
	Reverse	GGGTGCAATTACGTCACACC	
Gapdh	Forward	AGTGCCAGCCTCGTCTCATA	51
	Reverse	ATCCGTTCACACCGACCTTC	

Apoptosis detection by ELISA

Ovarian DNA fragmentation was measured using a Cell Death Detection ELISA Kit (Roche 11,544,675,001). In brief, frozen ovaries were snap-frozen in liquid nitrogen and crushed by a ceramic pestle. Then the tissue was homogenized in incubation buffer 50 times the volume of the ovary weight. The homogenate was then centrifuged at 20,000 g at 4 °C for 10 min. The supernatant was detected according to the manufacturer's protocols.

Statistical analysis

Data analysis was performed with SPSS 18.0 software. The continuous data were expressed as means ± standard deviation (SD). The Student's t-test was used to compare the differences between two groups. One-way analysis of variance (ANOVA) was used for comparisons among multiple groups. Categorical data were presented as frequency and percentage, and the between-group

differences were assessed using the chi-square test or Fisher's exact test as appropriate. $P < 0.05$ was considered statistically significant.

Abbreviations

ZYP	Zishen Yutai Pill
DOR	Diminished ovarian reserve
TGs	Tripterygium Glycosides tablets suspension
pZP3	Zona pellucida protein 3 peptides
CFA	Complete Freund's Adjuvant
FICA	Freund's Incomplete Adjuvant
AMH	Anti-Mullerian hormone
DHEA	Dehydroepiandrosterone
AFC	Antral follicle count
SART CORS	Society for Assisted Reproductive Technology Clinic Outcomes Reporting System
HRT	Hormone replacement therapy
ART	Assisted reproductive technology
TCM	Traditional Chinese Medicine
PFA	Paraformaldehyde
H&E	Hematoxylin and eosin
PCR	Polymerase chain reaction
FPKM	Fragments per kilobase of exon model per million mapped fragments
DEGs	Differentially expressed genes
KEGG	Kyoto encyclopedia of genes and genomes
GAPDH	Allogeneic glyceraldehyde-3-phosphate dehydrogenase
E2	Estradiol
FSH	Follicle-stimulating hormone
LH	Luteinizing hormone
mRNA	Messenger RNA
Pik3r5	Phosphoinositide-3-kinase regulatory subunit 5
Rxra	Retinoid X receptor alpha
Nr4a1	Nuclear receptor subfamily 4 group A member 1
Gnb3	G protein subunit beta 3
Tcl1a	T-cell leukemia/lymphoma 1A
Hsp90aa1	Heat shock protein 90 alpha family class A member 1
Bcl6	B-cell CLL/lymphoma 6B
Abtb2	Ankyrin repeat and BTB domain containing 2
PI3K	Phosphatidylinositol 3-kinase
AKT	Protein Kinase B
ELISA	Enzyme-linked immunosorbent assay

Acknowledgements
The authors appreciated the help from Jiewen Zhou in revising the manuscript.

Authors' contributions
J.C. and N.W. designed the study, performed the experiments, analyzed the data and wrote the draft. Z.P., X.P., N.Ni. and Q.D. performed the experiments. Q.G., Q.H. designed the study. J.C. and N.W. evaluated the quality of the whole study and drafted the manuscript. All authors reviewed the manuscript.

Funding
This work was supported by Department of Science and Technology of Guangdong Province (No. 2021B1212050018).

Data availability
No datasets were generated or analysed during the current study.

Declarations

Competing interests
The authors declare no competing interests.

Received: 16 September 2024 Accepted: 10 March 2025
Published online: 24 March 2025

References

1. Zhu Q, Li Y, Ma J, Ma H, Liang X. Potential factors result in diminished ovarian reserve: a comprehensive review. J Ovarian Res. 2023;16(1):208.
2. Lew R. Natural history of ovarian function including assessment of ovarian reserve and premature ovarian failure. Best Pract Res Clin Obstet Gynaecol. 2019;55:2–13.
3. Chen J, Kong X, Luan Z, Qiu Y, Chen S, Li Ling J, Gong Y. The effects of growth hormone on the outcomes of in vitro fertilization and embryo transfer in age-grouped patients with decreased ovarian reserve: a prospective cohort study. Front Endocrinol (Lausanne). 2024;15:1457866.
4. Qiu J, Dong M, Zhou F, Li P, Kong L, Tan J. Associations between ambient air pollution and pregnancy rate in women who underwent in vitro fertilization in Shenyang. China Reprod Toxicol. 2019;89:130–5.
5. Zhou Z, Li Y, Ding J, Sun S, Cheng W, Yu J, Cai Z, Ni Z, Yu C. Chronic unpredictable stress induces anxiety-like behavior and oxidative stress, leading to diminished ovarian reserve. Sci Rep. 2024;14(1):30681.
6. Xavier MJ, Salas-Huetos A, Oud MS, Aston KI, Veltman JA. Disease gene discovery in male infertility: past, present and future. Hum Genet. 2021;140(1):7–19.
7. Scheffer JB, Carvalho RF, Aguiar APS, Machado IJM, Franca JB, Lozano DM, Fanchin R. Which ovarian reserve marker relates to embryo quality on day 3 and blastocyst; age, AFC, AMH? JBRA Assist Reprod. 2021;25(1):109–14.
8. Guo Y, Jiang H, Hu S, Liu S, Li F, Jin L. Efficacy of three COS protocols and predictability of AMH and AFC in women with discordant ovarian reserve markers: a retrospective study on 19,239 patients. J Ovarian Res. 2021;14(1):111.
9. D'Alonzo M, Bounous VE, Villa M, Biglia N. Current Evidence of the Oncological Benefit-Risk Profile of Hormone Replacement Therapy. Medicina (Kaunas). 2019;55(9):573.
10. Zhang QL, Lei YL, Deng Y, Ma RL, Ding XS, Xue W, Sun AJ. Treatment Progress in Diminished Ovarian Reserve: Western and Chinese Medicine. Chin J Integr Med. 2023;29(4):361–7.
11. Zhang C, Xu X. Advancement in the treatment of diminished ovarian reserve by traditional Chinese and Western medicine. Exp Ther Med. 2016;11(4):1173–6.
12. Conforti A, Carbone L, Di Girolamo R, Iorio GG, Guida M, Campitiello MR, Ubaldi FM, Rienzi L, Vaiarelli A, Cimadomo D, et al. Therapeutic management in women with a diminished ovarian reserve: a systematic review and meta-analysis of randomized controlled trials. Fertil Steril. 2025;123(3):457–76.
13. Cameron CR, Cohen S, Sewell K, Lee M. The Art of Hormone Replacement Therapy (HRT) in Menopause Management. J Pharm Pract. 2024;37(3):736–40.
14. Zhang J, Jia H, Diao F, Ma X, Liu J, Cui Y. Efficacy of dehydroepiandrosterone priming in women with poor ovarian response undergoing IVF/ICSI: a meta-analysis. Front Endocrinol (Lausanne). 2023;14:1156280.
15. Ma Q, Shen M, Wu J, Ye C, Tan Y. Mechanism Research of DHEA Treatment Improving Diminished Ovarian Reserve by Attenuating the AMPK-SIRT1 Signaling and Mitophagy. Reprod Sci. 2024;31(7):2059–72.
16. Naik S, Lepine S, Nagels HE, Siristatidis CS, Kroon B, McDowell S. Androgens (dehydroepiandrosterone or testosterone) for women undergoing assisted reproduction. Cochrane Database Syst Rev. 2024;6(6):CD009749.
17. Romanski PA, Bortoletto P, Malmsten JE, Tan KS, Spandorfer SD. Pregnancy outcomes after oral and injectable ovulation induction in women with infertility with a low antimullerian hormone level compared with those with a normal antimullerian hormone level. Fertil Steril. 2022;118(6):1048–56.
18. Kool EM, Bos AME, van der Graaf R, Fauser B, Bredenoord AL. Ethics of oocyte banking for third-party assisted reproduction: a systematic review. Hum Reprod Update. 2018;24(5):615–35.
19. Liu W, Chen Q, Liu Z, Weng Z, Nguyen TN, Feng J, Zhou S. Zihuai recipe alleviates cyclophosphamide-induced diminished ovarian reserve via suppressing PI3K/AKT-mediated apoptosis. J Ethnopharmacol. 2021;277:113789.
20. Zhang X, Zhang L, Xiong L, Liu X, Zhang J, Yu F, Li Y, Chang W, Chen W. Kuntai capsule for the treatment of diminished ovarian reserve: A systematic review and meta-analysis of randomized controlled trials. J Ethnopharmacol. 2024;329: 118167.
21. Maharajan K, Xia Q, Duan X, Tu P, Zhang Y, Liu K. Therapeutic importance of Zishen Yutai Pill on the female reproductive health: A review. J Ethnopharmacol. 2021;281: 114523.

22. Zhou L, Huang Q, Wang R, Zhou J, Ma A, Chong L, Wu Y, Wang Y, Xu L, Chen Y, et al. Reproductive Toxicity of Zishen Yutai Pill in Rats: The Fertility and Early Embryonic Development Study (Segment I). Evid Based Complement Alternat Med. 2016;2016:3175902.
23. Zhou L, Zhou J, Jiang J, Yang Y, Huang Q, Yan D, Xu L, Chai Y, Chong L, Sun Z. Reproductive toxicity of ZishenYutai pill in rats: Perinatal and postnatal development study. Regul Toxicol Pharmacol. 2016;81:120–7.
24. Cavalcante MB, Sampaio OGM, Camara FEA, Schneider A, de Avila BM, Prosczek J, Masternak MM, Campos AR. Ovarian aging in humans: potential strategies for extending reproductive lifespan. Geroscience. 2023;45(4):2121–33.
25. Chen X, Hao C, Deng W, Bai H, Li Y, Wang Z, Shi Y, Zhang H, Zhu Y, Zhang H, et al. Effects of the Zishen Yutai Pill Compared With Placebo on Live Births Among Women in a Fresh Embryo Transfer Cycle: A Randomized Controlled Trial. Obstet Gynecol. 2022;139(2):192–201.
26. Xu X, Tan Y, Jiang G, Chen X, Lai R, Zhang L, Liang G. Effects of Bushen Tianjing Recipe in a rat model of tripterygium glycoside-induced premature ovarian failure. Chin Med. 2017;12:10.
27. Ai A, Xiong Y, Wu B, Lin J, Huang Y, Cao Y, Liu T. Induction of miR-15a expression by tripterygium glycosides caused premature ovarian failure by suppressing the Hippo-YAP/TAZ signaling effector Lats1. Gene. 2018;678:155–63.
28. Ma WR, Tan Y. The Effect and Mechanism of Hyperin on Ovarian Reserve of Tripterygium Glycosides-Induced POI Mice. Sichuan Da Xue Xue Bao Yi Xue Ban. 2021;52(3):458–66.
29. Hu F, Zhou X, Jiang Y, Huang X, Sheng S, Li D. Effect of Myrcene on Th17/Treg Balance and Endocrine Function in Autoimmune Premature Ovarian Insufficiency Mice through the MAPK Signaling Pathway. Protein Pept Lett. 2022;29(11):954–61.
30. Dilaver N, Pellatt L, Jameson E, Ogunjimi M, Bano G, Homburg R. H DM, Rice S: The regulation and signalling of anti-Mullerian hormone in human granulosa cells: relevance to polycystic ovary syndrome. Hum Reprod. 2019;34(12):2467–79.
31. Bedenk J, Vrtacnik-Bokal E, Virant-Klun I. The role of anti-Mullerian hormone (AMH) in ovarian disease and infertility. J Assist Reprod Genet. 2020;37(1):89–100.
32. Ma M, Chen XY, Li B, Li XT. Melatonin protects premature ovarian insufficiency induced by tripterygium glycosides: role of SIRT1. Am J Transl Res. 2017;9(4):1580–602.
33. Liu D, Tu X, Huang C, Yuan Y, Wang Y, Liu X, He W. Adoptive transfers of CD4(+) CD25(+) Tregs partially alleviate mouse premature ovarian insufficiency. Mol Reprod Dev. 2020;87(8):887–98.
34. Li HX, Shi L, Liang SJ, Fang CC, Xu QQ, Lu G, Wang Q, Cheng J, Shen J, Shen MH. Moxibustion alleviates decreased ovarian reserve in rats by restoring the PI3K/AKT signaling pathway. J Integr Med. 2022;20(2):163–72.
35. Bagavant H, Sharp C, Kurth B, Tung KS. Induction and immunohistology of autoimmune ovarian disease in cynomolgus macaques (Macaca fascicularis). Am J Pathol. 2002;160(1):141–9.
36. Lawrence J, Nho R. The Role of the Mammalian Target of Rapamycin (mTOR) in Pulmonary Fibrosis. Int J Mol Sci. 2018;19(3):778.
37. Andrade GM, da Silveira JC, Perrini C, Del Collado M, Gebremedhn S, Tesfaye D, Meirelles FV, Perecin F. The role of the PI3K-Akt signaling pathway in the developmental competence of bovine oocytes. PLoS ONE. 2017;12(9): e0185045.
38. Liu M, Qiu Y, Xue Z, Wu R, Li J, Niu X, Yuan J, Wang Y, Wu Q. Small extracellular vesicles derived from embryonic stem cells restore ovarian function of premature ovarian failure through PI3K/AKT signaling pathway. Stem Cell Res Ther. 2020;11(1):3.
39. Li L, Ning N, Wei JA, Huang QL, Lu Y, Pang XF, Wu JJ, Zhou JB, Zhou JW, Luo GA, et al. Metabonomics Study on the Infertility Treated With Zishen Yutai Pills Combined With In Vitro Fertilization-embryo Transfer. Front Pharmacol. 2021;12: 686133.
40. Yamochi T, Kaneita Y, Akiyama T, Mori S, Moriyama M. Adenovirus-mediated high expression of BCL-6 in CV-1 cells induces apoptotic cell death accompanied by down-regulation of BCL-2 and BCL-X(L). Oncogene. 1999;18(2):487–94.
41. Roy A, Pahan K. Ankyrin repeat and BTB/POZ domain containing protein-2 inhibits the aggregation of alpha-synuclein: implications for Parkinson's disease. FEBS Lett. 2013;587(21):3567–74.
42. Lee TI, Young RA. Transcriptional regulation and its misregulation in disease. Cell. 2013;152(6):1237–51.
43. Gong Y, Hu N, Ma L, Li W, Cheng X, Zhang Y, Zhu Y, Yang Y, Peng X, Zou D, et al. ABTB2 Regulatory Variant as Predictor of Epirubicin-Based Neoadjuvant Chemotherapy in Luminal A Breast Cancer. Front Oncol. 2020;10: 571517.
44. Li F, Zhou D, Ge Z, Wei Q. Pharmacological study on the mechanism of Zishen Yutai pill in the treatment of decreased ovarian reserve function. Shanxi Traditional Chinese Medicine. 2023;39(04):57–61.
45. Li XF, Wang ZQ, Xu HY, Liu H, Sheng Y, Xu J, Li YM, Lian F. Effects of Zishen Yutai Pills on in vitro Fertilization-Embryo Transfer Outcomes in Patients with Diminished Ovarian Reserve: A Prospective, Open-Labeled, Randomized and Controlled Study. Chin J Integr Med. 2023;29(4):291–8.
46. Yu M, Tang L, Sun X, Zhao J: Evaluation of Diminished Ovarian Reserve Animal Models Based on Clinical Disease-syndrome Characteristics of Traditional Chinese Medicine and Western Medicine. Chinese Journal of Experimental Traditional Medical Formulae 2025:1–11.
47. Hu X, Pan Q. Clinical observation of Zishen Yutai pill combined with acupuncture in the treatment of decreased ovarian reserve. Journal of Practical Traditional Chinese Medicine. 2022;38(12):2056–8.
48. Dong B, Wang Q. Clinical efficacy of Zishen Yutai pill in the treatment of decreased ovarian reserve function with spleen-kidney deficiency. China Practical Medicine. 2021;16(26):177–9.
49. Zhang H, Luo Q, Lu X, Yin N, Zhou D, Zhang L, Zhao W, Wang D, Du P, Hou Y, et al. Effects of hPMSCs on granulosa cell apoptosis and AMH expression and their role in the restoration of ovary function in premature ovarian failure mice. Stem Cell Res Ther. 2018;9(1):20.
50. Cora MC, Kooistra L, Travlos G. Vaginal Cytology of the Laboratory Rat and Mouse: Review and Criteria for the Staging of the Estrous Cycle Using Stained Vaginal Smears. Toxicol Pathol. 2015;43(6):776–93.
51. Chen S, Zhou Y, Chen Y, Gu J. fastp: an ultra-fast all-in-one FASTQ preprocessor. Bioinformatics. 2018;34(17):i884–90.

Publisher's Note